Fabrication and Properties of High Performance PEEK/Si_3N_4 Nanocomposites

V. Balaji,[1] A. N. Tiwari,[2] R. K. Goyal[3]

[1]*Materials Science Division, National Aerospace Laboratory, Bangalore 560 017, Karnataka, India*
[2]*Department of Metallurgical Engineering and Materials Science, Indian Institute of Technology Bombay, Mumbai 400 076, Maharashtra, India*
[3]*Department of Metallurgy and Materials Science, College of Engineering, Pune 411 005, Maharashtra, India*

Received 2 September 2009; accepted 9 March 2010
DOI 10.1002/app.32750
Published online 27 July 2010 in Wiley Online Library (wileyonlinelibrary.com).

ABSTRACT: The crystallization, morphology, microhardness, scratch hardness, dynamic modulus, and wear behavior of high performance poly(ether-ether-ketone) (PEEK) matrix nanocomposites reinforced with 0 to 30 wt % silicon nitride (Si_3N_4) nanoparticles were reported. The crystallinity of PEEK nanocomposites increases at 2.5 wt % Si_3N_4 but, thereafter it decreases with increasing Si_3N_4 content due to the hindrance to the ordering of PEEK chains. The crystallization peak temperature and crystallization onset temperature increases by 14°C for 10 wt % nanocomposite. The melting temperature does not vary significantly with Si_3N_4 content. SEM shows almost uniform distribution of Si_3N_4 in the PEEK matrix. The Vickers microhardness and scratch hardness increases significantly up to 10 wt % Si_3N_4 content.The dynamic modulus of nanocomposites increases below and above T_g of PEEK. The specific wear rate of nanocomposites with 2.5 wt % Si_3N_4 is reduced significantly and it is lowest at 10 wt % Si_3N_4. However, the coefficient of friction of nanocomposites is more than that of pure PEEK. © 2010 Wiley Periodicals, Inc. J Appl Polym Sci 119: 311–318, 2011

Key words: nanocomposites; crystallinity; hardness; wear rate; PEEK

INTRODUCTION

Poly(ether-ether-ketone) (PEEK), a semicrystalline thermoplastic engineering polymer, exhibits excellent thermal, mechanical, chemical, and electrical properties. It is an attractive material for journal bearings and piston rings under various loading conditions as it is comparatively fatigue resistance and exhibits a low creep rate at higher temperatures.[1–4] Its low coefficient of friction and comparatively low wear rate than other polymers has attracted its use for as a rubbing surface material in machinery.[5] Its wear resistance (inverse of wear rate) has been significantly improved by incorporating fibers, such as carbon fiber,[3,6] carbon nano fibers,[4] and particles, such as CuS,[7] Si_3N_4,[8] SiO_2,[9] SiC,[10] and ZrO_2.[11] The improvement in wear resistance of composites was attributed to the smoothing of the counter surface, the developing of a transfer film, improved hardness and modulus. However, the smoothness, hardness, and stiffness[12–13] are not only the factors controlling the wear behavior, but also the nature and stability of the transfer film and its adhesion to the counter surface affects the wear properties.[13–15] Moreover, the wear resistance significantly depends on many factors, such as dispersion state, size, volume fraction, and type of nano sized particles, and crystallinity of the polymer matrices.[16–17]

Recently, Goyal et al.[18,19] have demonstrated the effect of micro and nano particles of Al_2O_3 on wear resistant of PEEK matrix composites**.** They reported that nanoparticles were more effective than micro particles in improving wear resistance of PEEK composites prepared and tested under the similar conditions.[18–19] Wang et al.[8] have studied the wear behavior of Si_3N_4 filled PEEK nanocomposites using block-on-ring machine.[8] However, authors have not discussed crystallinity, scratch hardness and dynamic modulus of this nanocomposite, which are important factors to know about the wear mechanisms of composites. In view of above, PEEK matrix nanocomposites were fabricated by incorporating Si_3N_4 nanoparticles ranging from 0 to 30 wt % using hot pressing technique. The crystallization behavior, morphology, microhardness, scratch hardness, dynamic modulus, wear and friction properties of nanocomposites were evaluated using differential scanning calorimeter, scanning electron microscopy, Vickers microhardness, scratch hardness tester, dynamic mechanical analyzer, and pin-on-disk wear tester, respectively. Moreover, optical microscope

Correspondence to: R. K. Goyal (E-mail: rkgoyal72@yahoo.co.in).

was used to study nature of transfer film developed on counter surface during sliding wear using pin-on disk tester.

EXPERIMENTAL

Materials

The commercial PEEK (GATONE^{TM}, Grade 5300PF) was used as matrix. The silicon nitride (Si_3N_4) nanoparticles purchased from Aldrich Chemical Company was used as reinforcement. The density and BET specific surface area of Si_3N_4 is 3.44 g/cm^3 and 103–123 m^2/g, respectively. As received ethanol of Merck grade was used for homogenizing the Si_3N_4 nanoparticles and the PEEK powder. Figure 1 shows TEM image of Si_3N_4 powder, which shows that the shape of the nanoparticles is almost spherical with particle size less than 50 nm.

Fabrication of the PEEK/Si_3N_4 nanocomposites

PEEK matrix nanocomposites reinforced with Si_3N_4 up to 30 wt % loading were fabricated using the method described in our previous article.[1] The dried powder of Si_3N_4 was suspended in an ethanol using ultrasonic bath for 30 min and PEEK powder was well mixed with it through magnetic stirring. The resultant slurry was dried in an oven at 120°C to remove the excess ethanol. The dried mixed powder was filled in a steel die and hot pressed at 350°C and 15 MPa. Fabricated samples were coded as NC-*X*, where *X* indicates wt % of the Si_3N_4 in the PEEK matrix.

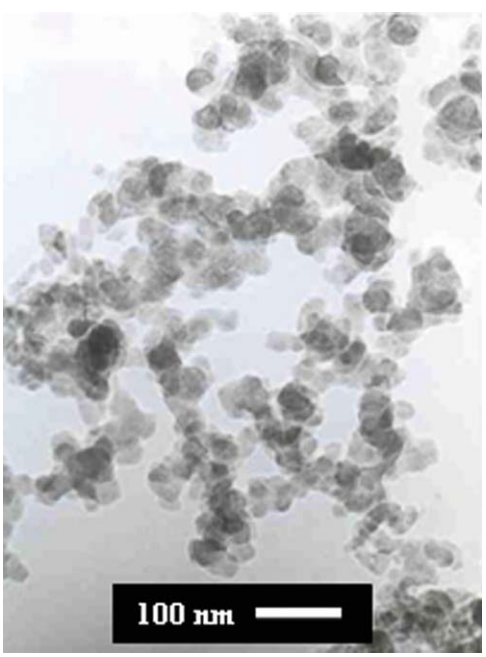

Figure 1 TEM image of Si_3N_4 powder, scale bar: 100 nm. [Color figure can be viewed in the online issue, which is available at wileyonlinelibrary.com.]

Characterization methods

Morphological examination

To study the degree of dispersion of Si_3N_4 in the matrix and worn surfaces, samples were coated with gold using a gold sputter coater [Polaron SC 7610] and studied using SEM (Hitachi S-3400N). The transfer films formed between the pin and counter surface were examined by optical microscopy (Nikon).

Differential scanning calorimetry

The normalized heat of crystallization, degree of crystallinity, melting point, and crystallization peak temperature of PEEK and nanocomposites were determined using DSC (Du Pont Instruments 910 DSC). The samples placed in an aluminum pan was first heated from 30 to 400°C at a heating rate 10°C/min and soaked isothermally at 400°C for 1 min to allow complete melting of the samples. The samples were then cooled to temperatures below 120°C at a cooling rate 10°C/min. Each sample is subjected to single heating and cooling cycles under a dry nitrogen purge, and data are recorded during the first heating and cooling cycle. The crystallinity percentage (χ_c) of PEEK constituent in nanocomposite was determined by $\chi_c = \Delta H_c \times 100/(\Delta H_c^{\circ}. W)$, where, ΔH_c° is the heat of crystallization (130 J/g) for 100% crystalline PEEK,[1] ΔH_c is the heat of crystallization for nanocomposite and W is the mass fraction of PEEK in the nanocomposites.

Mechanical properties (microhardness, scratch hardness, and dynamic modulus)

The microhardness was measured using Vickers hardness tester (DVK-2S, Japan) under load of 50 g and dwell time of 15 sec. An average of six readings was reported as the microhardness. For the measurement of scratch hardness of PEEK and nanocomposites, the diamond indentor was held on a pivoted beam to position it orthogonally on the flat substrate as shown in Figure 2. The sample was secured on the stage which can be manually adjusted along X- and Y- axes. A fixed normal load (62.08 g) was used and the scratch is made on the samples by manually moving the stage containing the sample at a controlled slow rate past the indentor. The width of the permanent scratch created by the indentor was measured using an optical microscope. The scratch hardness (H_s) can be calculated, to a good approximation, by $H_s = 8 \cdot W/\pi \cdot d^2$, where, W is the normal load and d is the scratch width. The dynamic modulus of PEEK and nanocomposites were determined

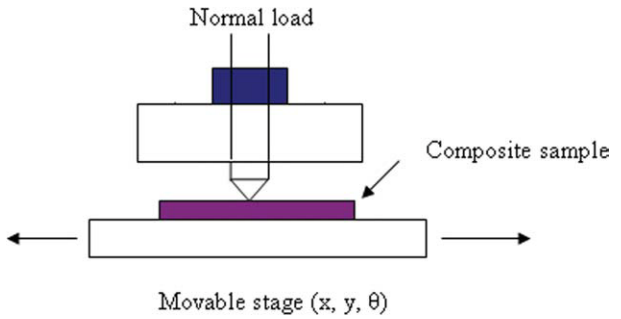

Figure 2 Scratch hardness apparatus. [Color figure can be viewed in the online issue, which is available at wileyonlinelibrary.com.]

in the three point bending mode using dynamic mechanical analyzer (PerkinElmer DMA 7e) from 30 to 250°C at a heating rate of 5°C/min and a frequency of 1 Hz. The tests were carried out in argon atmosphere under static load of 110 mN and a dynamic load of 100 mN.

Wear rate and coefficient of friction

Wear rate and coefficient of friction were conducted on a pin-on-disk wear tester at a sliding speed of 1.0 m/s and nominal pressure of 0.2 to 0.8 MPa. The tests were conducted for a total sliding distance of 15 km for low pressures and 9 km for higher pressures. The EN-24 steel disc of diameter 76.48 mm and thickness 5 mm was employed as the counter surface. It was heat treated to harden to HRC4. The disc surface was polished with abrasive paper to a surface roughness of $R_a = 0.21$ μm. The surface of the counter surface and pin was cleaned thoroughly with cotton dipped in acetone. The wear tests were carried out at a relative humidity of 52 ± 2% and 31 ± 2°C condition. The decrease in the height of the composite pin disc was measured using a digital micrometer with a precision of 1 μm. The tests were performed till two successive equal height reductions (i.e. wear rates) were attained. The dimensionless wear rate of the samples can be given by, $h/s = W_s . p$, where, h is the height of the sample removed, s is the sliding distance, and p is the nominal pressure. The specific wear rate (W_s) can be determined by the slope of the line between the h/s and p.

RESULTS AND DISCUSSION

Morphological examination

Figure 3 shows SEM images of the PEEK/Si_3N_4 nanocomposites. It can be seen from Figure 3(a,b) that nanoparticles are well dispersed in the matrix of NC-5 and there is no observable agglomeration of the nanoparticles. In case of NC-10 as shown in Figure 3(c,d) nanoparticles are still well dispersed but some agglomerates having sizes about 100 nm can be seen. Figure 3(e,f) show large aggregate and severe porosities of few microns size in NC-20 and NC-30 nanocomposites, respectively. This is due to the decrease in interparticle distances as the nanoparticles loading in nanocomposites increases and it results in clusters or agglomerates of Si_3N_4 nano particles due to the weak Van der Waal forces.

Differential scanning calorimetry (DSC)

From the heating and cooling DSC curves, the thermal properties are calculated and tabulated in Table I. The crystallinity percentage of PEEK (χ_c) is calculated with 130 cal/g as the heat of crystallization for the 100% crystalline PEEK.[1] During cooling, the crystallinity increases for NC-2 (2.5 wt % Si_3N_4) but, thereafter it decreases with increasing Si_3N_4 content as shown in Table I. It increased from 28.3% for pure PEEK to 31.2% for NC-2 and then dropped to 23.9% for NC-10 and 16.65 for NC-30. The decrease in crystallinity for nanocomposites at higher loading indicates that the nanoparticles have imposed hindrance to the PEEK macromolecular chains in getting into an ordered crystalline structure. The peak temperature of crystallization (T_c) for pure PEEK was 260°C and it increased by 14 to 274°C for NC-10. The increase in T_c with increasing Si_3N_4 indicates that the nanoparticles acted as a heterogenous nucleation sites and hence, enhanced the rate of PEEK crystallization. As the nanoparticles dispersed quite efficiently, which provide numerous nucleation sites for the PEEK chains to crystallize. But, with increase in the nucleation sites, the nanoparticles also hinder the molecules to crystallize and hence the decrease in crystalline fraction despite increase in the crystallization temperature. The crystallization onset temperature (T_{on}) was 267°C for pure PEEK and was above 280°C for NC-10 as shown in Table 1. The melting temperature, T_m, has not varied much with the Si_3N content. It has remained at 335 ± 3°C for the entire composition range. However, the variation in T_m about 2–3°C of nanocomposites was observed similar to those with nano silica or nano alumina.[20]

Mechanical properties

Vickers microhardness

Figure 4 shows the microhardness of the nanocomposites as a function of Si_3N_4 content in the PEEK matrix. It can be seen that microhardness increases significantly up to 10 wt % Si_3N_4. This improvement is attributed to higher microhardness (1700 kg/mm^2) of Si_3N_4 compared to PEEK, which resist penetration of indentation in the matrix. However, above 10 wt % Si_3N_4 the increase in hardness is not significant.

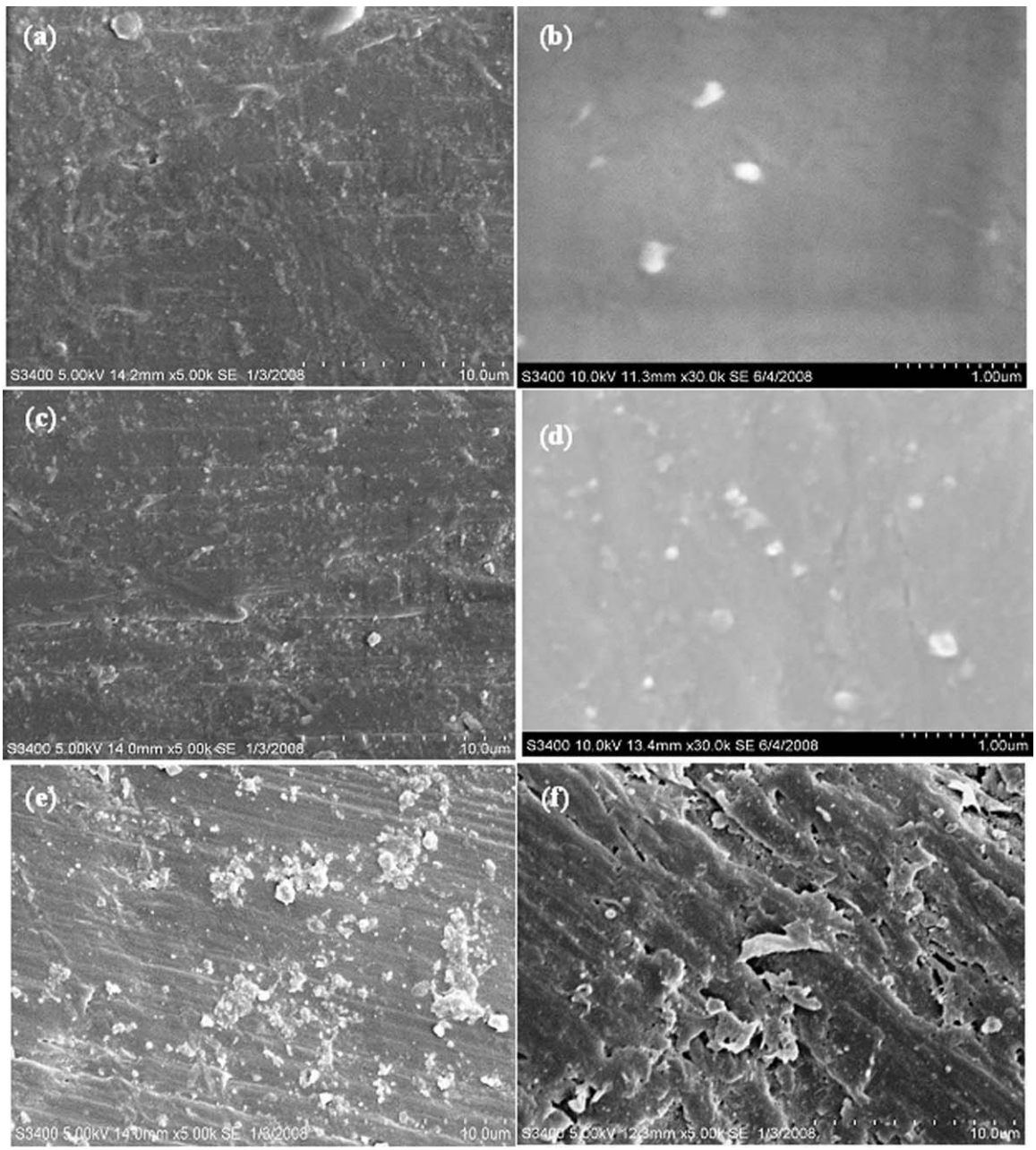

Figure 3 SEM images of polished nanocomposites of (a,b) NC-5, (c,d) NC-10, (e) NC-20, and (f) NC-30; scale bar 10 μm (a,c,e,f) and 1 μm (b,d).

TABLE I
Thermal Property of PEEK/Si_3N_4 Nanocomposites Determined by DSC

Sample code	% Si_3N_4 in PEEK		Normalized heat of crystallization (J/g)	Crystallinity (%)	T_{on} (°C)	T_c (°C)	T_m (°C)
	By wt.	By vol.					
NC-0	0	0	36.79	28.30	267.1	260.0	334.3
NC-2	2.5	0.96	40.65	31.26	274.0	268.2	335.8
NC-5	5	1.95	34.40	26.46	282.3	271.9	337.2
NC-10	10	4.03	31.12	23.94	281.0	274.2	335.8
NC-20	20	8.63	27.95	21.50	268.3	260.5	334.1
NC-30	30	13.93	21.60	16.61	265.4	255.5	332.2

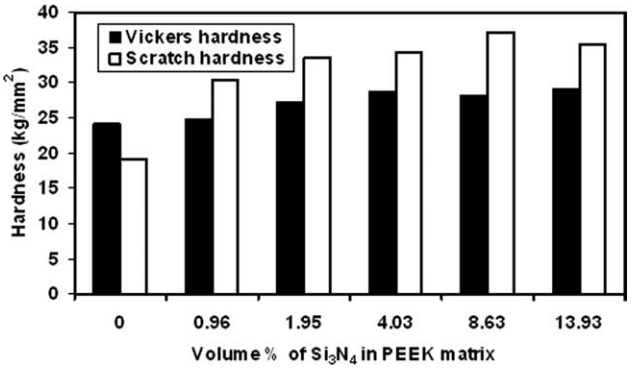

Figure 4 Microhardness and Scratch hardness of PEEK/Si_3N_4 nanocomposites.

This might be attributed to the decreased crystallinity as confirmed from DSC and presence of porosities in nanocomposites with higher Si_3N_4 loading.

Scratch hardness

The variation of the scratch hardness of nanocomposites with Si_3N_4 content is also shown in Figure 4. The scratch hardness test being a dynamic test shows that the scratch hardness has significantly increased even for low dispersoid loading. It increases from 19 kg/mm^2 for the pure PEEK to 30 kg/mm^2 or NC-2 nanocomposite, i.e., 60% improvement in scratch hardness at 2.5 wt % Si_3N_4. The increase in the crystallinity of PEEK and the uniform dispersion of nano Si_3N_4 particles might have imparted a very high scratch resistance of nanocomposite at lower filler content. This indicates that the improvement in crystallinity of PEEK might be an important factor in improving the scratch hardness.[21] Moreover, the higher hardness of Si_3N_4 compared to pure PEEK and the change in morphology of PEEK matrix in the adjacent region of the reinforcement can also contribute to the improved scratch hardness.[22] However, the increase in the scratch hardness is not proportionate to the Si_3N_4 content at higher loading. For example, it increased from 30 kg/mm^2 for NC-2 to 37 kg/mm^2 for NC-20. The presence of agglomerations/porosities and decreased crystallinity of PEEK for nanocomposites containing more than 10 wt % Si_3N_4 probably resulted in only a marginal increase in scratch hardness.

Storage modulus

Figure 5 shows the storage modulus as a function of temperature for the pure PEEK and nanocomposites containing 2.5 wt % (NC-2) and 5 wt % Si_3N_4 (NC-5). As expected, the storage modulus increases at all temperatures with increasing Si_3N_4 content in the

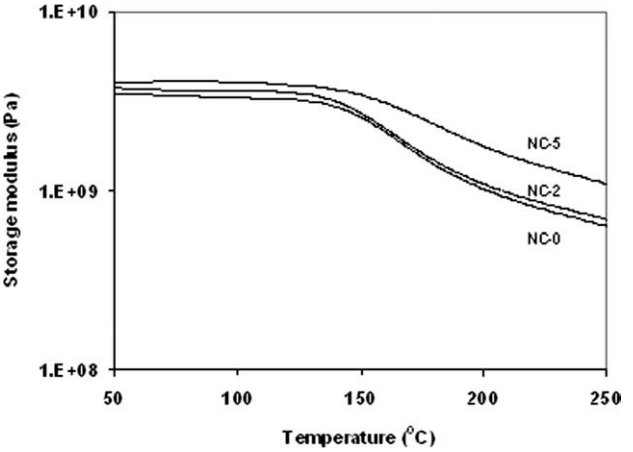

Figure 5 Storage modulus versus temperature of PEEK/Si_3N_4 nanocomposites.

PEEK matrix. The modulus of nanocomposites exhibits fairly stable values up to 100°C. The modulus increases due to the high modulus of Si_3N_4 compared to pure PEEK and from the interface formed between the Si_3N_4 and the matrix. However, the modulus of pure PEEK and nanocomposites decreases with increasing temperatures particularly above 100°C. This is due to the fact that molecular relaxation increases with increasing temperature. A similar trend is observed for Al_2O_3 filled PEEK nanocomposites.[18]

Wear rate and coefficient of friction

The specific wear rate of PEEK and its nanocomposites is shown in Figure 6. The specific wear rate of nanocomposites decreases with increasing Si_3N_4 content. It is lowest for the 10 wt % nanocomposite. The significant decrease in wear rate can be attributed to the increased hardness, scratch hardness, and dynamic modulus of nanocomposites. However, on further increasing Si_3N_4, it increases abruptly despite higher hardness of NC-20 than pure PEEK. Thus,

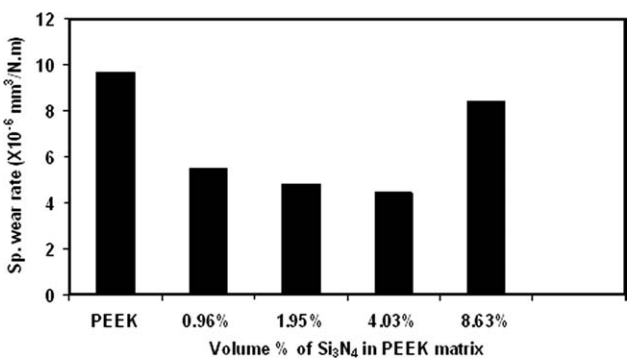

Figure 6 Specific wear rate of PEEK/Si_3N_4 nanocomposites.

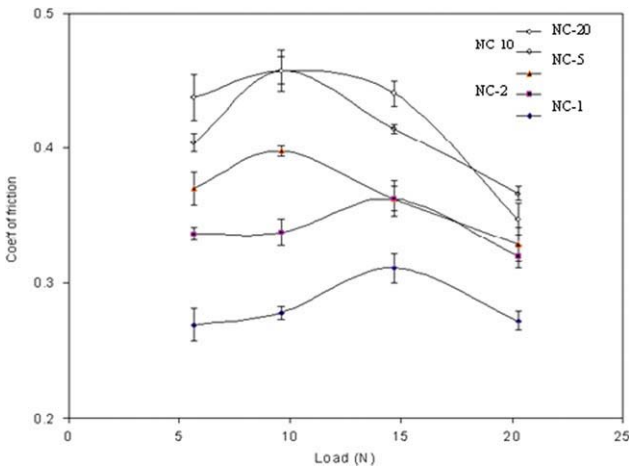

Figure 7 Coefficient of friction as a function of load for PEEK/Si_3N_4 nanocomposites. [Color figure can be viewed in the online issue, which is available at wileyonlinelibrary.com.]

the hardness alone does not decide the wear rate of nanocomposites containing higher loading, though it influences particularly in the composites with low loading. There is some mechanism like transfer film that play important role.

Figure 7 shows the coefficient of friction (μ) of PEEK and its nanocomposites as a function of the load. The coefficient of friction is the least for pure PEEK and it has increased with both the load as well as the Si_3N_4 content. For a load of 14.7 *N*, the μ increases from 0.31 to 0.44 as Si_3N_4 content increases from 0 to 20 wt %. This is similar to that of Al_2O_3 filled PEEK nanocomposite.[18] As the Si_3N_4 nano particles increases there will be more microploughing and third body abrasion taking place which will increase the friction between the pin and the counter surface. And because of this increased friction more and more metallic particles get into the wear debris, which are detected by the EDS.

SEM study of the worn surfaces of nanocomposites

Figure 8 shows SEM of the worn surfaces of pure PEEK and its nanocomposite pins. The worn surface of pure PEEK shows signs of adhesive wear which is caused by the removal of flaky or lamellae like debris from the pin surface. Therefore adhesive wear is the dominant wear mechanism for pure PEEK. In case of NC-10, microploughing is also seen along with adhesive wear. The microploughing arises due to the third body abrasion resulting from the hard

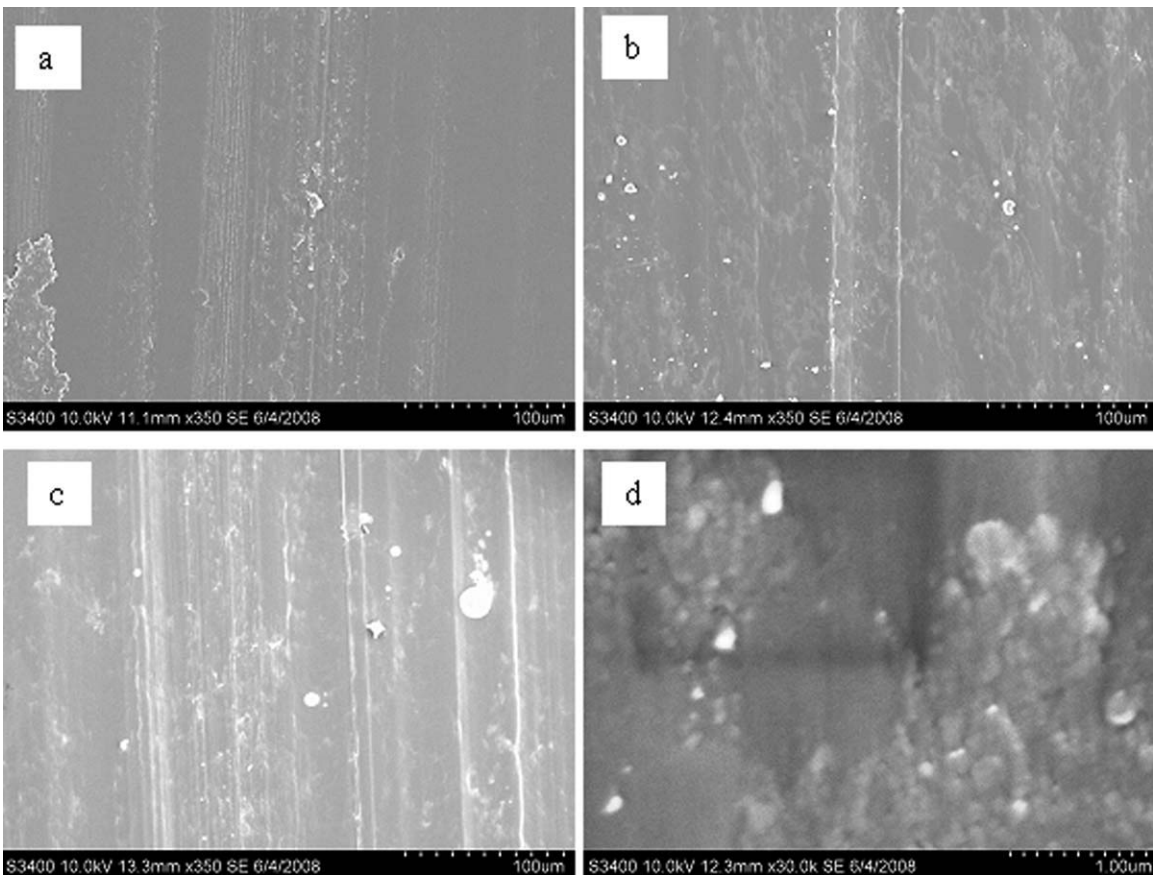

Figure 8 SEM of worn surface of pins of; (a) pure PEEK, (b) NC-10, and (c and d) NC-20.

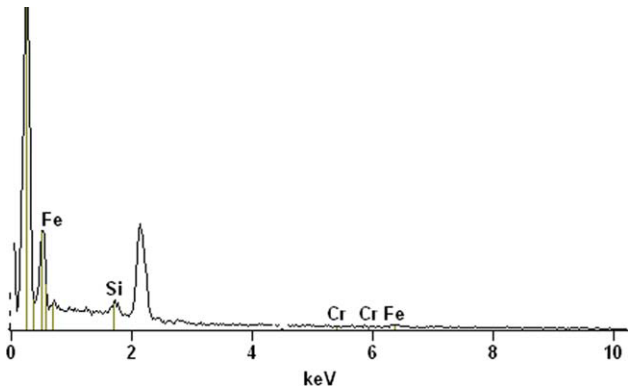

Figure 9 EDS of wear debris of NC- nanocomposite. [Color figure can be viewed in the online issue, which is available at wileyonlinelibrary.com.]

nano particles getting loosened from the matrix. This results in the abrasion of even hard metallic disc. Though, both mechanisms of wear were seen in the NC-20, the transfer film was not continuous and the Si_3N_4 nano particles could be observed in the micrograph at a higher magnification in Figure 8(d). The worn surface of NC-20 contains wear particles from the steel counter surface which was confirmed from energy dispersive spectroscopy (EDS) as shown in Figure 9. The presence of Fe and Cr elements in worn surface confirms the abrasion of counter surface by NC-20 nanocomposite pin.

Optical microscopy of transfer films

Figure 10 shows the nature of transfer film formed on the steel counter surface due to sliding wear of nanocomposites. Figure 10(a) shows the as polished initial surface of the counter surface. Figure 10(b–d) shows the transfer films developed after 3 km sliding by pure PEEK, NC-10, and NC-20 nanocomposites, respectively. Pure PEEK forms a continuous loosely transfer film, which covers the troughs and asperities of the counter surface. A uniform transfer film can be seen in the case of NC-10, therefore exhibits a low specific wear rate. But for NC-20, the transfer film is only partial on the counter surface, possibly because of poor adhesive strength of the film with the counter surface. At a higher dispersant loading, particle-particle interaction is substantial leading to aggregation and this hinders the formation of continuous transfer film. The increase in the Si_3N_4 nano particles up to 10 wt % decreases the specific wear rate as the transfer film is thin, tenacious, and coherent. The microhardness also increases substantially from 24 kg/mm^2 for PEEK to 29 kg/mm^2 for NC-10. Above 10 wt % loading,

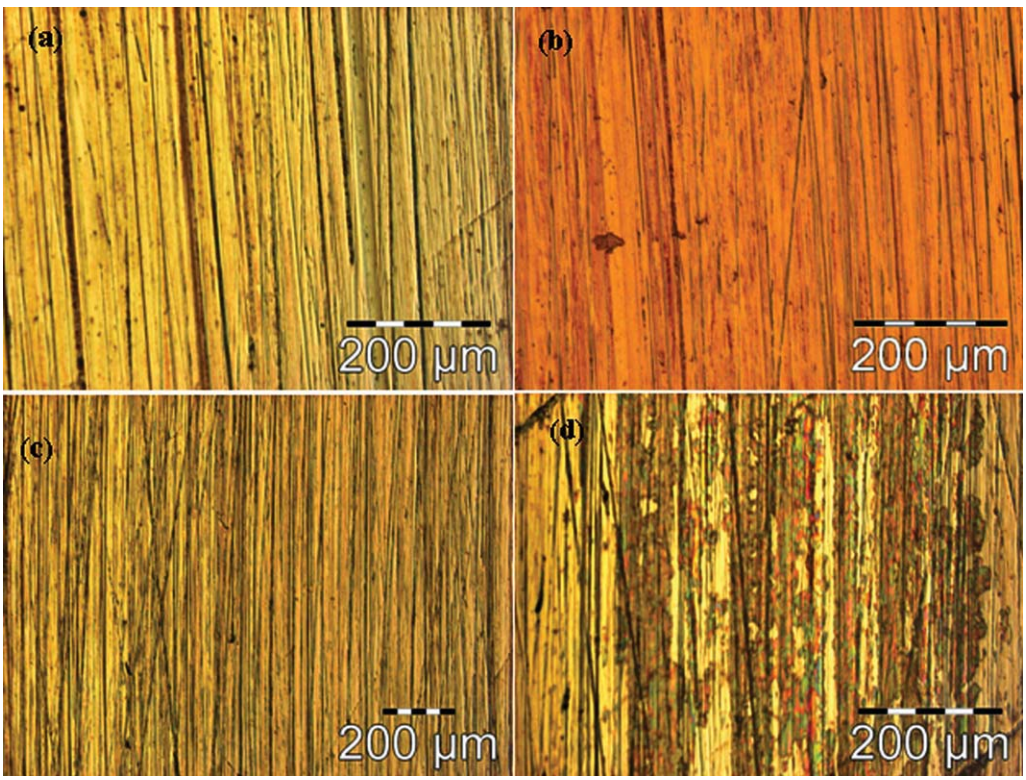

Figure 10 Optical micrographs of transfer films developed on steel counter surface during sliding wear for; (a) polished counter surface, (b) pure PEEK, (c) NC-10, and (d) NC-20. [Color figure can be viewed in the online issue, which is available at wileyonlinelibrary.com.]

Si_3N_4 agglomerates hinder the formation of a continuous transfer film and thereby increases wear rate.

CONCLUSIONS

The PEEK matrix nanocomposites reinforced with varying loading of Si_3N_4 nanoparticles were successfully fabricated by hot pressing. The presence of Si_3N_4 acts as a strong nucleating agent which results in improvement in crystallinity of PEEK at 2.5 wt % Si_3N_4 content but decreases degree of crystallization above it. The crystallization peak temperature, crystallization onset temperature, Vickers hardness, dynamic modulus, and scratch hardness were improved significantly up to 10 wt %. These improvements may be attributed to the uniform distribution of Si_3N_4 nanoparticles in the PEEK matrix as confirmed from SEM images. The wear rate of nanocomposite with 2.5 wt % was decreased significantly and of nanocomposite with 10 wt % was the lowest. However, above 10 wt %, properties were not improved significantly due to the formation of aggregates. The SEM images of the nanocomposite pins and optical microscopy observation of the wear tracks indicate that the formation of a good adherent transfer film play an important role in improving wear resistance.

We thank Gharda Chemicals, India for providing PEEK powder for this work.

References

1. Goyal, R. K.; Negi, Y. S.; Tiwari, A. N. J Appl Polym Sci 2006, 100, 4623.
2. Frederic, N. C. Thermoplastic Aromatic Polymer Composites; Butterworth Heinemann Ltd: Oxford, 1992.
3. Lu, Z. P.; Friedrich, K. Wear 1995, 181, 624.
4. Werner, P.; Altstädt, V.; Jaskulka, R.; Jacobs, Q.; Sandler, J. K. B.; Shaffler, M. S. P.; Windle, A. H. Wear 2004, 257, 1006.
5. Yamamoto, Y.; Hashimoto, M. Wear 2004, 257, 181.
6. Hanchi, J., Jr; Eiss, N. S. Wear 1997, 203, 380.
7. Bahadur, S.; Gong, D. Wear 1992, 154, 151.
8. Wang, Q. H.; Xu, J.; Shen, W.; Liu, W. Wear 1996, 196, 82.
9. Wang, Q.; Xue, Q.; Shen, W. Tribol Int 1997, 30, 193.
10. Wang, Q. H.; Xu, J.; Shen, W.; Xue, Q. Wear 1997, 209, 316.
11. Wang, Q. H.; Xu, J.; Liu, H.; Shen, W.; Xu, J. Wear 1996, 198, 216.
12. Schwartz, C. J.; Bahadur, S. Wear 2000, 237, 261.
13. Bahadur, S.; Sunkara, C. Wear 2005, 258, 1411.
14. Sawyer, W. G.; Freudenberg, K. D.; Bhimaraj, P.; Schadler, S. Wear 2003, 254, 573.
15. Li, F.; Hu, K.; Li, J.; Zhao, B. Wear 2002, 249, 877.
16. Durand, J. M.; Vardavouliar, M.; Jeandin, M. Wear 1995, 181, 833.
17. Bhimaraj, P.; Burris, D. L.; et al. Wear 2005, 258, 1437.
18. Goyal, R. K.; Tiwari, A. N.; Negi, Y. S. Mater Sci Eng A 2008, 486, 602.
19. Goyal, R. K.; Tiwari, A. N.; Mulik, U. P.; Negi, Y. S. J Appl Polym Sci 2008, 110, 3379.
20. Kuo, M. C.; Tsai, C. M.; Huang, J. C.; Chen, M. Mater Chem Phys 2005, 90, 185.
21. Stuart, B. H.; Briscoe, B. J. Polym Bull 1996, 36, 767.
22. Dasari, A.; Rohrmann, J.; Misra, R. D. K. Mater Sci Eng A 2004, 364, 357.